M1/M2 Macrophage Skewing is Related to Reduction in Types I, V, and VI Collagens with Aging in Sun-Exposed Human Skin

Satoshi Horiba[1], Munetaka Kawamoto[1], Ryozo Tobita[1], Ryota Kami[1], Yuki Ogura[1] and Junichi Hosoi[1]

Sun-exposed, aged human skin is fragile because of collagen fragmentation and loss. We recently reported that the balance of M1 and M2 macrophages is associated with chronic inflammation and related inflammaging in sun-exposed human skin. In this study, we analyzed its role in the maintenance of collagen matrix formation by performing histological analyses of human facial skin. In addition, RNA sequencing, protein assays, and functional assays revealed the details of the mechanism. The number of M2 macrophages was positively correlated with the abundance of type I collagen, whereas the M1/M2 ratio was negatively correlated with the abundance of type V and VI collagen, which are the essential minor collagens required for collagen assembly in the skin; however, there was no correlation with type III collagen. Furthermore, M2 macrophages induced the expression of the proteins required for the assembly of collagen fibrils, suggesting that the M1/M2 balance controls not only the quantity but also the quality of the collagen matrix. Indeed, M1 macrophages induced abnormal collagen fibrils consisting of types I, V, and VI collagens. Our results demonstrate the relationship between the M1/M2 balance and the dysregulation of collagen homeostasis in photoaged skin and suggest the possible involvement of macrophages in skin photoaging.

JID Innovations (2023);**3:**100222 doi:10.1016/j.xjidi.2023.100222

INTRODUCTION

Because the skin is directly affected by UV irradiation, sun-induced skin aging is called photoaging and is superimposed with aging caused by the passage of time (chronological aging) (El-Domyati et al., 2002; McCabe et al., 2020). Photoaging is characterized by reduced production and increased fragmentation of the dermal extracellular matrix because of chronic inflammation (Gordon and Brieva, 2012; Kligman, 1969). Type I collagen fibrils are strongly affected by photoaging in the skin (Fisher et al., 1997; Fligiel et al., 2003). UV irradiation inhibits the expression of TGF-b type II receptor and induces downregulation of type I collagen in dermal fibroblasts (Rittié and Fisher, 2002). In addition, UV irradiation induces chronic inflammation and upregulates the expression and activation of matrix metalloproteinase (MMP) in dermal fibroblasts, resulting in type I collagen fragmentation (Rittié and Fisher, 2015; Sonoki et al., 2018). Furthermore, in photoaged skin, dermal fibroblasts lack a direct association with surrounding collagen fibrils, resulting in the loss of mechanical force and collagen synthesis as well as an increase in matrix-degrading metalloproteinases (Fisher et al., 2014; Quan et al., 2013; Varani et al., 2002; Xia et al., 2013). These findings indicate that a reduction in collagen fibrils in photoaged skin reduces collagen synthesis, increases collagen fibril fragmentation, and causes the skin to become fragile. Therefore, many studies have focused on the direct effect of UV on the homeostasis of type I collagen in dermal fibroblasts to investigate the mechanism of photoaging in the skin; however, the effects of UV on the homeostasis of minor collagens, such as types V and VI collagens, have not been fully elucidated. Types V and VI collagens are essential minor collagens that stabilize the matrix of the dermis, especially at the papillary dermis, by binding with type I collagen fibrils as bridging molecules (Bonod-Bidaud et al., 2012).

Among immune cells in the skin, macrophages play key roles in wound healing, which has a remodeling phase that is essential for the dynamic assembly of collagen fibrils (Mahdavian Delavary et al., 2011). It has been reported that macrophages can be roughly divided into two subsets: M1 (proinflammatory) and M2 (anti-inflammatory) (Wynn and Vannella, 2016). We recently reported that the M1/M2 macrophage balance is altered with aging in sun-exposed skin, which induces chronic inflammation and related inflammaging (Horiba et al., 2022). However, the relationship between aging-related dysregulation of collagen homeostasis and a shift in the M1/M2 balance in sun-exposed skin has not been fully investigated.

In this study, we found that alterations in the M1/M2 balance were negatively correlated with the abundance of collagen in sun-exposed skin. We also observed that M1 cells induced MMPs, whereas M2 cells induced collagens and proteins that can control the assembly of collagen fibrils in dermal fibroblasts; therefore, a shift in the M1/M2 balance may affect not only the quantity but also the quality of collagen fibrils in photoaged skin.

[1]*MIRAI Technology Institute, Shiseido, Yokohama, Japan*

Correspondence: Satoshi Horiba, MIRAI Technology Institute, Shiseido, 1-2-11, Takashima, Nishi-ku, Yokohama 220-0011, Japan. E-mail: satoshi.horiba@shiseido.com

Abbreviations: MMP, matrix metalloproteinase; LPS, lipopolysaccharide; SHG, second harmonic generation

Received 17 November 2022; revised 4 July 2023; accepted 6 July 2023; accepted manuscript published online XXX; corrected proof published online XXX

Cite this article as: JID Innovations 2023;3:100222

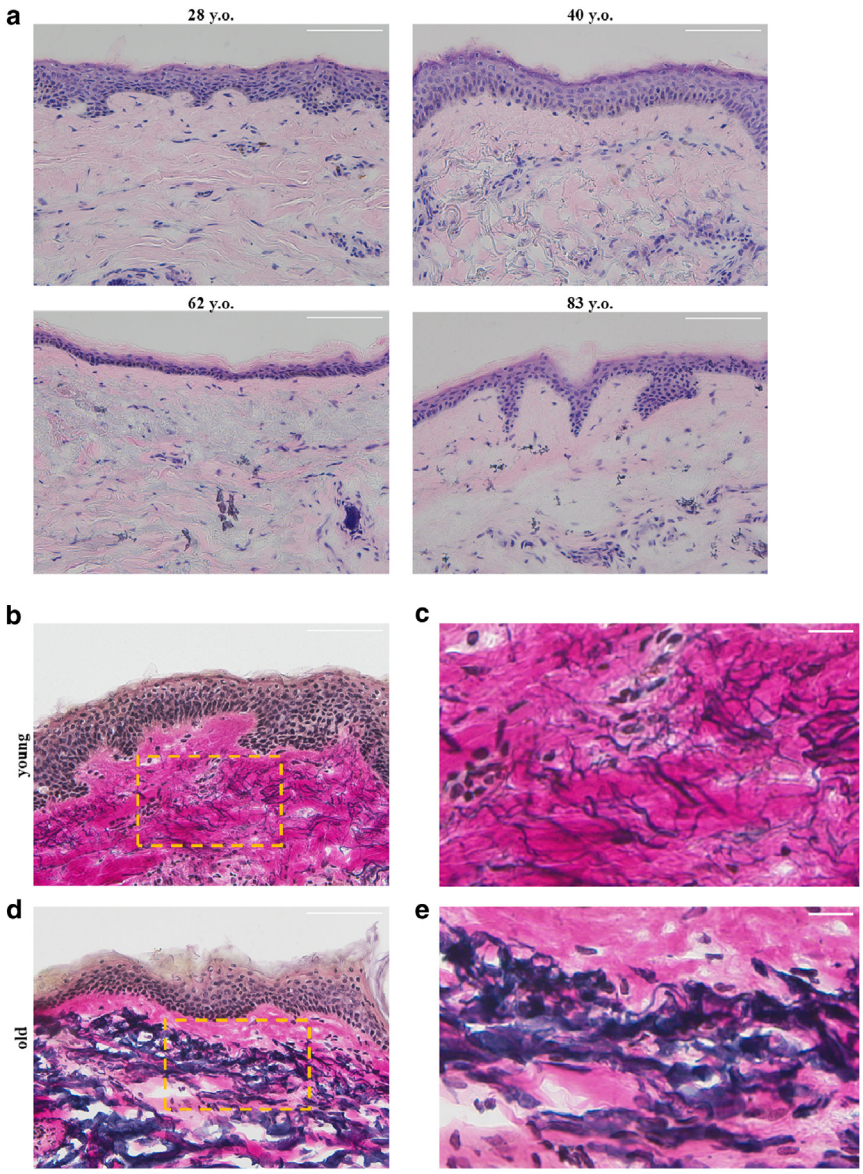

Figure 1. Immunohistochemistry of sun-exposed young and aged human skin. (**a**) Typical images of H&E staining. (**b**) Representative Elastica-Van Gieson staining of young skin. (**c**) Enlarged view of **b**. (**d**) Representative Elastica-Van Gieson staining of aged skin. (**e**) Enlarged view of **d**. Bar = 100 μm or 20 μm in the enlarged view. y.o., year old.

RESULTS

The M1/M2 balance is skewed in sun-exposed aged skin

To characterize the skin samples, we performed H&E staining and Elastica van Gieson staining and then scored the degree of solar elastosis (Figure 1a–e and Table 1). Next, to investigate the difference in the M1/M2 ratio between young and aged sun-exposed skin, we stained M1 and M2 macrophages and counted their numbers in the papillary dermis located within 200 μm of the epidermal border. We stained M1 macrophages with both CD86 and CD68, which are the major surface markers of human M1 macrophages and total human macrophages, respectively. The number of M1 macrophages increased with aging in sun-exposed skin, although the difference was not significant (Figure 2a and c). On the other hand, the number of M2 macrophages was significantly decreased with aging, as revealed by staining M2 macrophages with CD206, which is the major surface marker of human M2 macrophages, and CD68 ($P = 0.0089$, Mann–Whitney U test) (Figure 2b and d). In addition, the M1/M2 ratio was significantly increased ($P = 0.0028$, Mann–Whitney U test) (Figure 2e), indicating that the balance between M1 and M2 macrophages was altered with aging in sun-exposed skin. Furthermore, we found no significant relationship between the degree of solar elastosis and the number of M1 macrophages (Figure 2f); however, there was a significant negative relationship between the degree of solar elastosis and the number of M2 macrophages ($\rho = -0.7099$, $P = 0.0005$) (Figure 2g) and a significant positive relationship between the degree of solar elastosis and the M1/M2 ratio in the dermis ($\rho = 0.5092$, $P = 0.0219$) (Figure 2h). To test the significance of the scatter plots, Spearman's rank correlation coefficient was used. These results indicate that the number of M2 macrophages is related to solar elastosis.

Amount of type I collagen is related to the number of M2 macrophages in sun-exposed human skin

To examine whether the shift in the M1/M2 balance with aging affects collagen formation in the dermis of sun-exposed

Table 1. Skin Samples Characteristics

Age, y	Sex	Race[1]	Degree of Solar Elastosis[2]
25	Female	White	1+
27	Female	White	1+
27	Female	White	2+
28	Female	White	1+
33	Female	White	1+
35	Female	White	2+
38	Female	White	2+
39	Female	White	2+
40	Female	White	2+
43	Female	White	1+
62	Female	White	3+
63	Female	White	4+
66	Female	White	3+
69	Female	White	3+
70	Female	White	4+
75	Female	White	3+
76	Female	White	3+
83	Female	White	4+
83	Female	White	3+
88	Female	White	3+

Abbreviations: y, year.
[1]Race was determined by the supplier.
[2]Degree of solar elastosis was scored according to the criteria by Kligman (1969).

skin, we performed immunostaining for type I collagen. We analyzed the signal intensity of type I collagen in the papillary dermis located within 200 μm of the epidermal border, and it was significantly lower in photoaged skin ($P = 0.0011$, Mann–Whitney *U* test) (Figure 3a and b). In addition, we quantified second harmonic generation (SHG) signals from collagen in the same area and found that these signals were significantly decreased in photoaged skin ($P = 0.0147$, Mann–Whitney *U* test) (Figure 3c and d). Furthermore, we analyzed the relationship between the signal intensity of type I collagen or SHG signals and the number of M1 and M2 macrophages and the M1/M2 ratio in the papillary dermis. The signal intensity of type I collagen and SHG signals were not affected by the number of M1 macrophages (Figure 3e and h). However, there was a significant positive relationship between the signal intensity of type I collagen or SHG signals and the number of M2 macrophages ($\rho = 0.4962$, $P = 0.0261$ [Figure 3f]; $\rho = 0.4481$, $P = 0.0475$ [Figure 3i]). Furthermore, the signal intensity of type I collagen and the M1/M2 ratio tended to be negatively correlated, though the statistical *P*-value was 0.0798 ($\rho = -0.4009$, $P = 0.0798$) (Figure 3g). The SHG signals were not affected by the M1/M2 ratio (Figure 3j). To test the significance of the scatter plots, Spearman's rank correlation coefficient was used.

These results indicate that the number of M2 macrophages may affect the abundance of type I collagen in the papillary dermis.

M1 (lipopolysaccharide + IFN-γ) is involved in the regulation of type I collagen production in dermal fibroblasts

To investigate whether M1 or M2 macrophages affect the synthesis of type I collagen, we differentiated M1 macrophages and M2 macrophages from THP-1 cells and called them M1 (lipopolysaccharide [LPS] + IFN-γ) and M2 (IL-4 + IL-13). We cultured an ex vivo skin model with M1 (LPS + IFN-γ) and M2 (IL-4 + IL-13) (Figure 4a). The signal intensity of type I collagen in the papillary dermis was significantly lower in the presence of M1 (LPS + IFN-γ) than it was without macrophages ($P = 0.0281$, Friedman's test (Figure 4b and c). Furthermore, to examine the effect of both subsets of macrophages on the expression of type I collagen in detail, we cultured dermal fibroblasts with the supernatant from the M1 (LPS + IFN-γ) or M2 (IL-4 + IL-13) (Figure 4d). Staining for type I collagen revealed that the synthesis of type I collagen was decreased by the supernatant of M1 (LPS + IFN-γ) (Figure 4e). The expression of procollagen was quantified using an ELISA and found that the supernatant of M1 (LPS + IFN-γ) significantly decreased the expression of procollagen compared with the control ($P = 0.0394$, Kruskal–Wallis test) (Figure 4f). In addition, the expression of *COL1A1* and *COL1A2* mRNA ($P = 0.0051$, Kruskal–Wallis test [Figure 4g] and $P = 0.0051$, Kruskal–Wallis test [Figure 4h]) also decreased significantly. Furthermore, the mRNA expression of *MMP1* in dermal fibroblasts cultured with the supernatant of M1 (LPS + IFN-γ) increased significantly ($P = 0.0051$, Kruskal–Wallis test) (Figure 4i). These results indicate that M1 macrophages may have the ability to not only decrease the expression but also induce the fragmentation of type I collagen in dermal fibroblasts.

M1 (LPS + IFN-γ) induces the expression of MMPs, and M2 (IL-4 + IL-13) induces the expression of collagen and proteins that support collagen fiber formation in dermal fibroblasts

To understand why M1 and M2 macrophages affect the abundance of type I collagen, we performed a bulk RNA-sequencing analysis of the mRNA of dermal fibroblasts cultured with the supernatant of M1 (LPS + IFN-γ) or M2 (IL-4 + IL-13). As a result, 10,305 significantly differentially expressed genes between M1 (LPS + IFN-γ) and M2 (IL-4 + IL-13) were identified using the q-value ($q < 0.05$) as the threshold. Figure 5a shows the top 20 results of the enrichment analysis of the differentially expressed genes. The top three enriched terms were related to the extracellular matrix. This finding indicates that M1 and M2 macrophages have different functions, especially in maintaining the extracellular matrix. Among the top 20 results of the enrichment analysis (Figure 5a), we focused specifically on collagen, identifying collagen formation–related genes (R-HAS: 1474290; collagen formation) that were differentially expressed and drawing a heatmap (Figure 5b). M1 (LPS + IFN-γ) induced the expression of genes such as *MMP1*, *MMP3*, and *MMP9* that code for major MMPs in the skin (Figure 5b) ($q = 1.22e\text{-}09$ [Figure 5k], $q = 6.64e\text{-}14$ [Figure 5l], and $q = 5.02e\text{-}11$ [Figure 5m]), whereas M2 (IL-4 + IL-13) induced the expression of genes that are essential for the assembly, maturation, or maintenance of type I collagen, such as *PPIB* ($q = 1.26e\text{-}15$), *P4HB* ($q = 8.43e\text{-}16$), *SPARC* ($q = 2.01e\text{-}21$), lysyl oxidase gene *LOX* ($q = 1.61e\text{-}16$), *ACAN* ($q = 9.58e\text{-}18$), and *ADAMTS2* ($q = 9.42e\text{-}14$) (Figure 5b). In addition, M2 (IL-4 + IL-13) induced the expression of not only genes for type I collagen but also for types III, V, and VI collagens

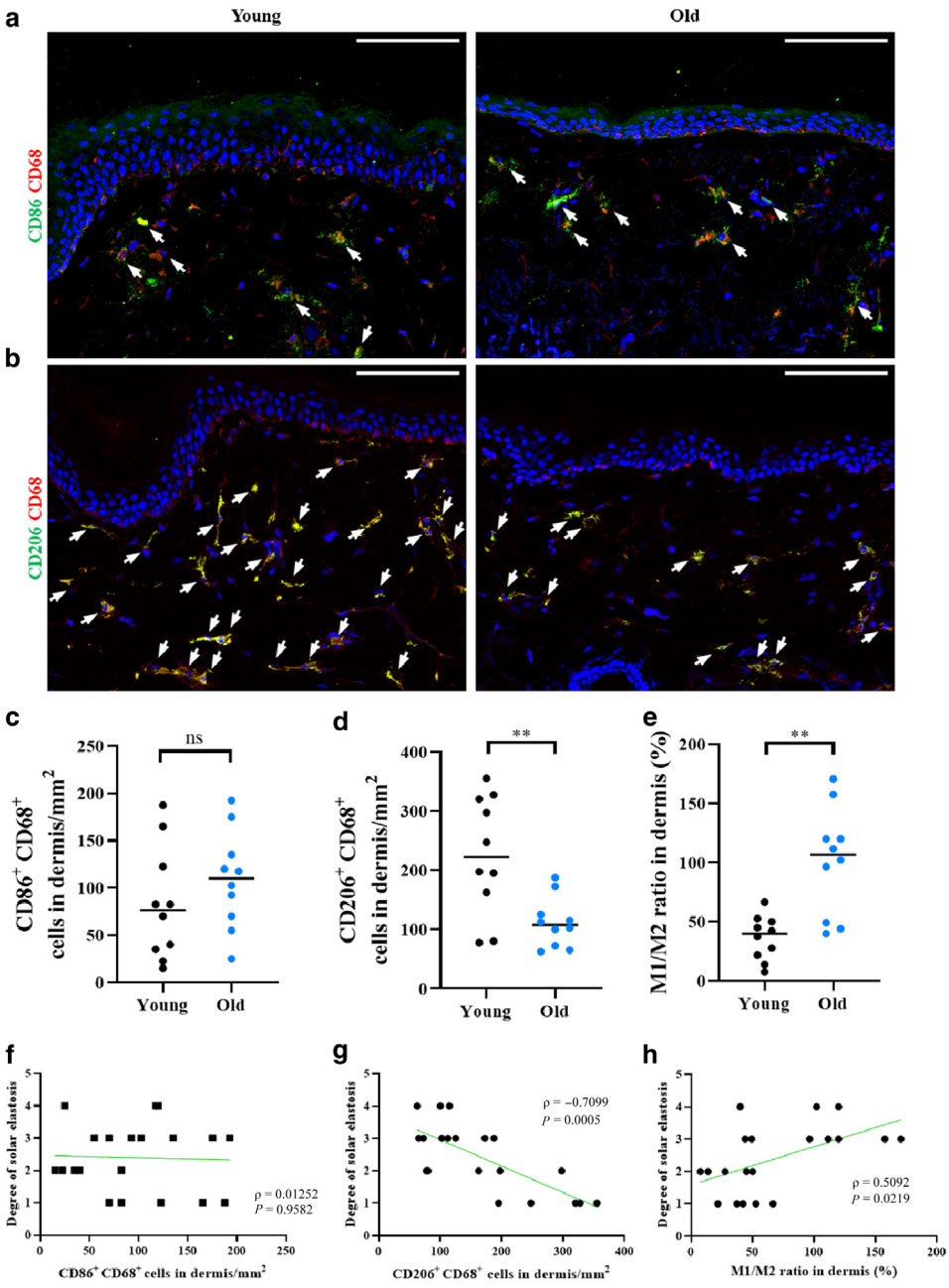

Figure 2. The number of M2 macrophages is decreased, and the M1/M2 ratio is skewed in aged skin. (**a**) Young (mean = 34.2 years) and aged (mean = 74.5 years) human skin samples were stained with anti-CD86 (green) and anti-CD68 (red) antibodies. The arrows indicate CD86+ CD68+ cells in the dermis. (**b**) Young (mean = 34.2 years) and aged (mean = 74.5 years) human skin samples were stained with anti-CD206 (green) and anti-CD68 (red) antibodies. The arrows indicate CD206+ CD68+ cells in the dermis. (**c**) Quantitation of CD86+ CD68+ cells/mm^2 in the dermis. (**d**) Quantitation of CD206+ CD68+ cells/mm^2 in the dermis. (**e**) Quantitation of the M1/M2 ratio (number of CD86+ CD68+ cells/number of CD206+ CD68+ cells) in the dermis. (**f**) Correlation between the degree of solar elastosis and the number of M1 macrophages in the papillary dermis of young and aged skin samples. (**g**) Correlation between the degree of solar elastosis and the number of M2 macrophages in the papillary dermis of young and aged skin samples. (**h**) Correlation between the degree of solar elastosis and the M1/M2 ratio in the papillary dermis of young and aged skin samples. Nuclei were stained with Hoechst (blue). n = 10 in both the young and aged groups. $^{**}P < 0.01$. The Mann–Whitney *U* test was used to test for significance. To test the significance of the scatter plots, Spearman's rank correlation coefficient was used. Bar = 100 μm. ns, not significant.

(q = 2.79e-07 [Figure 5c], q = 2.84e-12 [Figure 5d], q = 1.39e-15 [Figure 5e], q = 5.02e-08 [Figure 5f], q = 1.03e-11 [Figure 5g], q = 4.12e-07 [Figure 5h], q = 1.86e-06 [Figure 5i], and q = 2.18e-06 [Figure 5j]). Furthermore, to examine the effect of M1 (LPS + IFN-γ) and M2 (IL-4 + IL-13) on fibroblast proliferation, we analyzed the expression of genes that are known to be involved in fibroblast proliferation. We found that M2 (IL-4 + IL-13) induced the expression of *CD248* (q = 1.11e-10), which is known as an activation marker of mesenchymal lineage cells. Among the significantly altered genes, those related to types III, V, and VI collagens are highly expressed in the dermis and are also essential for maintaining and assembling type I collagen; therefore, we examined the relationship between M1 and M2 macrophages and these three collagen types.

The amount of types V and VI collagens is related to the M1/M2 ratio in sun-exposed human skin

To examine whether types III, V, and VI collagen are related to M1 and M2 macrophages in sun-exposed skin, we performed immunostaining for these three collagen types in the papillary dermis located within 200 μm of the epidermal border. The signal intensities of all three collagen types were significantly lower in photoaged dermis; this was especially true for types V and VI collagens ($P = 0.0355$, Mann–Whitney *U* test [Figure 6a and b]; $P < 0.0001$, Mann–Whitney *U* test [Figure 6c and d]; and $P = 0.0007$, Mann–Whitney *U* test [Figure 6e and f]). In addition, the signal intensities of these three collagen types were not affected by the number of M1 macrophages (Figure 6g, j, and m). Furthermore, the signal intensities of types V and VI

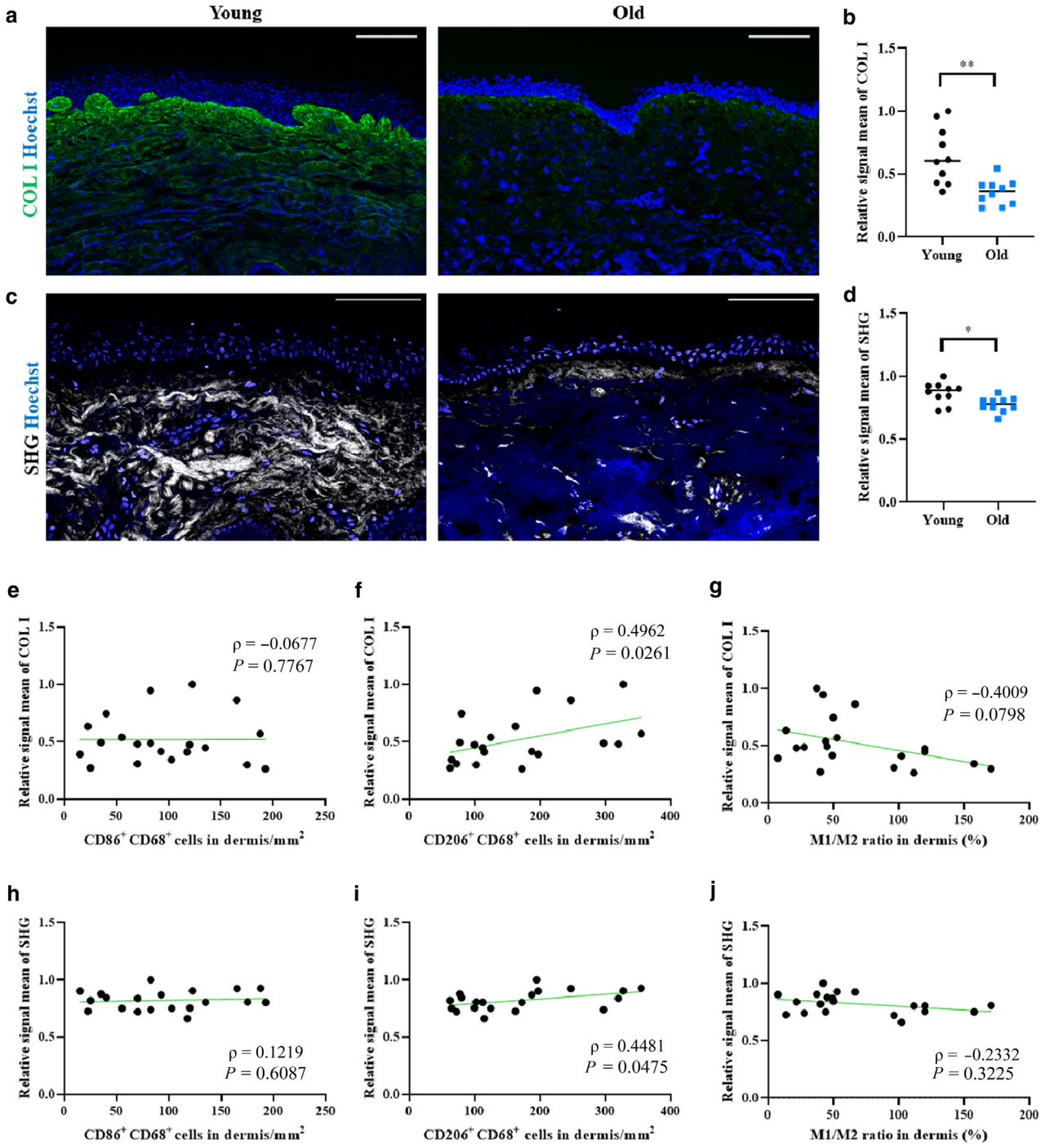

Figure 3. The amount of type I collagen is related to the number of M2 macrophages in sun-exposed human skin. (**a**) Young (mean = 34.2 years) and aged (mean = 74.5 years) human skin was stained with anti–type I collagen (green) antibodies. (**b**) Quantitation of the relative mean signal of type I collagen in the papillary dermis. (**c**) Representative SHG images of young skin and aged human skin. (**d**) Quantitation of the relative mean signal of SHG in the papillary dermis. (**e**) Correlation between the relative mean signal of type I collagen and the number of M1 macrophages in the papillary dermis of young and aged skin samples. (**f**) Correlation between the relative mean signal of type I collagen and the number of M2 macrophages in the papillary dermis of young and aged skin samples. (**g**) Correlation between the relative mean signal of type I collagen and the M1/M2 ratio in the papillary dermis of young and aged skin samples. (**h**) Correlation between the relative mean signal of SHG and the number of M1 macrophages in the papillary dermis of young and aged skin samples. (**i**) Correlation between the relative mean signal of SHG and the number of M2 macrophages in the papillary dermis of young and aged skin samples. (**g**) Correlation between the relative mean signal of SHG and the M1/M2 ratio in the papillary dermis of young and aged skin samples. Nuclei were stained with Hoechst (blue). n = 10 in both the young and aged groups. $*P < 0.05$ and $**P < 0.01$. The Mann–Whitney *U* test was used to test for significance. To test the significance of the scatter plots, Spearman's rank correlation coefficient was used. Bar = 100 μm. SHG, second harmonic generation.

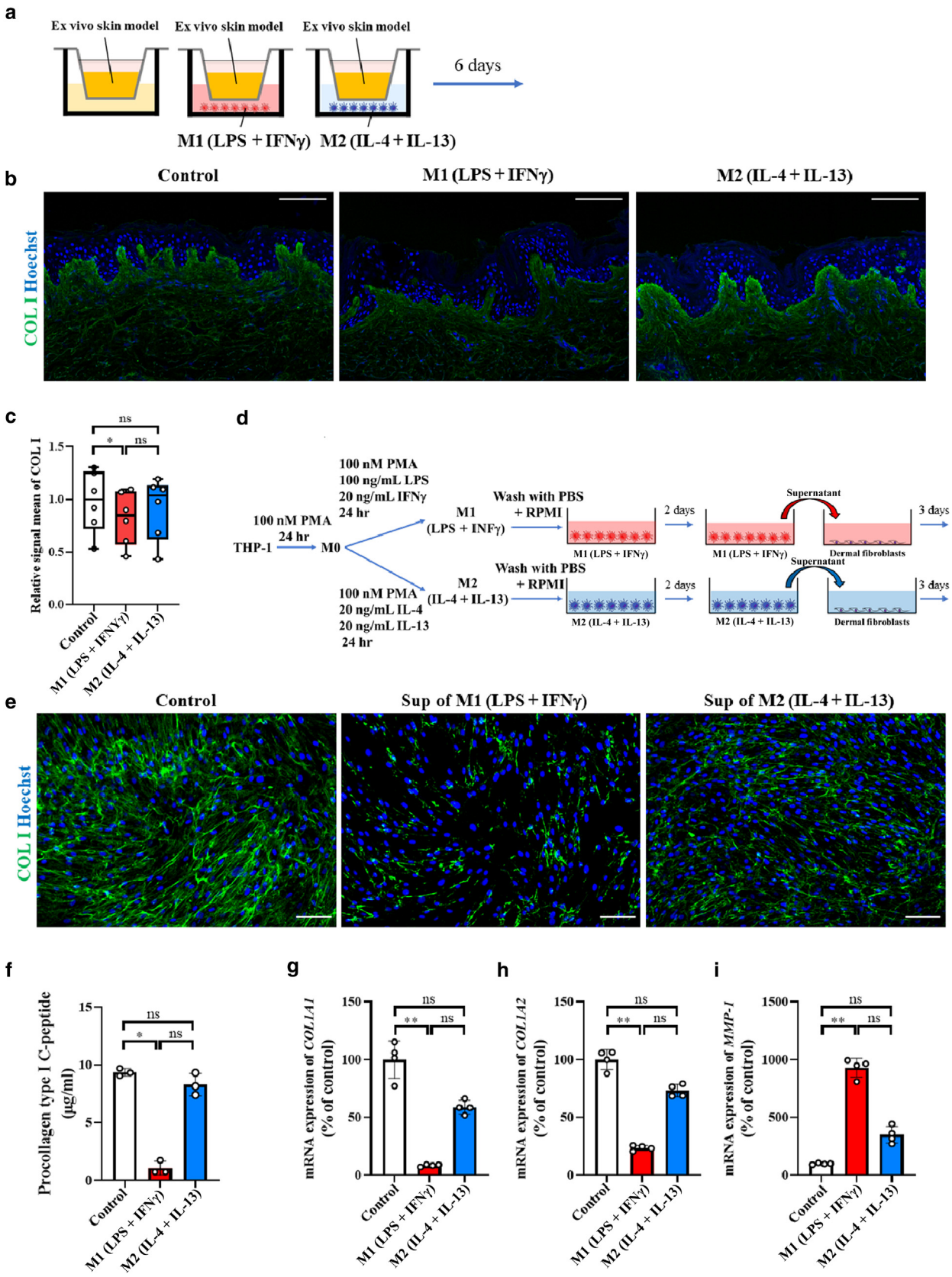

Figure 4. M1 (LPS + IFN-γ) is involved in the regulation of type I collagen production in dermal fibroblasts. (**a**) Experimental scheme for examining the effect of M1 (LPS + IFN-γ) and M2 (IL-4 + IL-13) on ex vivo skin models (aged 25−38 years; mean = 32.3 years) in vitro. (**b**) Representative samples showing immunofluorescence staining of type I collagen (green) in the ex vivo skin model. (**c**) Quantitation of the relative mean signal of type I collagen in ex vivo models. Each box shows the median (central horizontal line) and IQR, and whiskers represent the first and third quartiles of 1.5 × IQR. Nuclei were stained with Hoechst (blue). n = 6 for control, M1 (LPS + IFN-γ), and M2 (IL-4 + IL-13), and each dot in the bar charts represents a separate experiment (different donors).

collagens and the number of M2 macrophages tended to be negatively correlated, though the statistical *P*-values were 0.0519 and 0.0565, respectively ($\rho = 0.4406$, $P = 0.0519$ [Figure 6k] and $r = 0.4331$, $P = 0.0565$ [Figure 6n]). Moreover, there was a significant negative relationship between the signal intensities of types V and VI collagens and the M1/M2 ratio ($\rho = -0.5197$, $P = 0.0188$ [Figure 6l] and $\rho = -0.4573$, $P = 0.0426$ [Figure 6o]). However, we did not find a relationship between the signal intensity of type III collagen and the number of M2 macrophages or the M1/M2 ratio (Figure 6h and i). These results indicate that the M1/M2 ratio may influence the abundance of types V and VI collagens and that the relationship with types V and VI collagens is stronger than that with type III collagen in sun-exposed dermis.

Collagen fibril formation is regulated by the M1/M2 balance of macrophages

Finally, to investigate the effects of M1 and M2 macrophages on the synthesis and assembly of collagen fibrils consisting of types I, V, and VI collagens, dermal fibroblasts were cultured with the supernatant of M1 (LPS + IFN-γ) and M2 (IL-4 + IL-13), and types I, V, and VI collagens were stained (Figure 7a, b, d, e, g, and h). In addition, we analyzed the fluorescence colocalization of the characteristic area using scatterplots of pixel intensity (Figure 7c, f, and i). Dermal fibroblasts cultured with control medium or M2 (IL-4 + IL-13) supernatant synthesized sharp collagen fibrils, and types V and VI collagens colocalized with and supported type I collagen (Figure 7a, b, g, and h). However, dermal fibroblasts cultured with M1 (LPS + IFN-γ) supernatant synthesized fragmented collagen fibrils (Figure 7d and e). In addition, in some characteristic areas, collagen colocalization of types I, V, and VI was different in fibroblasts cultured with M1 (LPS + IFN-γ) supernatant compared with that of the control (Figure 7c and f). These results indicate that the M1/M2 balance may affect not only the quantity but also the quality of collagen fibrils.

DISCUSSION

Type I collagen is the most abundant and structurally important collagen in the dermis. Many researchers have reported the mechanisms of photoaging through which UV irradiation induces the reduced expression and degradation of type I collagen through dermal fibroblasts (Cole et al., 2018). However, the effect of immune cells on the alteration of type I collagen—and even more so on the alteration of minor collagens such as types V and VI collagens, which are essential for supporting collagen fibrils with type I collagen in photoaged human skin—has not yet been fully analyzed. In this study, we analyzed the relationship between macrophages and collagen in photoaging and found that the M1/M2 balance in the skin may control the abundance of types I, V, and VI collagens and the assembly of collagen fibrils in the dermis. These results, together with our previous report (Horiba et al., 2022) that shows the relationship between the M1/M2 balance and senescence of dermal fibroblasts in photoaged skin, provide a hypothesis for the mechanism of photoaging that is based on the skewing of the macrophage balance in human skin. We hypothesize that in addition to the direct effect of UV radiation on the matrix formation of dermal fibroblasts that causes photoaging in sun-exposed skin, the skewing of the macrophage balance induced by UV radiation causes chronic inflammation and contributes to the acceleration of dermal fibroblast aging, which leads to collagen homeostasis dysfunction, resulting in the formation of wrinkles or sagging in the skin of the face.

To investigate the mechanisms through which the M1/M2 balance affects collagen homeostasis, bulk RNA-sequencing analysis was performed with cultured dermal fibroblasts incubated with the supernatant from differentiated M1 and M2 macrophages. We found that M1 macrophages induced the expressions of *MMP1*, *3*, and *9*, which are the major enzymes degrading type I collagen during photoaging (Pittayapruek et al., 2016). Meanwhile, M2 macrophages induced the expression of proteins that are essential for the assembly of collagen fibrils, such as *SPARC*, lysyl oxidase gene *LOX*, and *ADAMTS2*. SPARC is a matricellular protein, and it has been reported that *Sparc*-null mice exhibit decreased collagen fibril diameters and abnormalities in the dermis (Bradshaw et al., 2003). In addition, it has also been reported that SPARC regulates the processing of procollagen I and the assembly of collagen fibrils in dermal fibroblasts (Rentz et al., 2007). Similar to SPARC, lysyl oxidase plays a critical role in stabilizing collagen fibrils by initiating the formation of covalent cross-linkages (Kagan and Li, 2003). ADAMTS-2 is the major N-proteinase for procollagens, and *Adamts2*-knockout mice have fragile skin because of abnormal collagen fibrils caused by the excessive accumulation of procollagen I (Bekhouche and Colige, 2015). Our results, together with the reported findings, suggest that M2 macrophages induce the assembly of collagen fibrils and control collagen homeostasis in the skin. Indeed, during skin repair, it has been reported that CD206-positive M2-like macrophages control collagen fibril assembly (Knipper et al., 2015). Furthermore, in addition to supporting the assembly of collagen by these proteins, M2 cells induced the expression of not only type I but also types III, V, and VI collagens. Types III, V, and VI collagens are the major collagens in the dermis, and they coexist with type I collagen in collagen fibrils and support fibril structure and skin elasticity (Fleischmajer et al., 1990; Gelse et al., 2003); however, the

*$P < 0.05$. To test for the significance of the intensity of type I collagen, Friedman's test with multiple comparisons was used. Bar = 100 mm. (**d**) Experimental scheme for examining the effect of supernatants from M1 (LPS + IFN-γ) and M2 (IL-4 + IL-13) on dermal fibroblasts in vitro. (**e**) Representative immunofluorescence staining of type I collagen (green) in dermal fibroblasts. (**f**) Quantitation of the procollagen type I C-peptide in the medium of dermal fibroblasts that were cultured with macrophage supernatant. Each dot in the bar charts represents a triplicate of the same plate. (**g**) Quantitation of the mRNA expression of *COL1A1* in dermal fibroblasts cultured with macrophage supernatant. Each dot in the bar charts represents a quadruplicate of the same plate. (**h**) Quantitation of the mRNA expression of *COL1A2* in dermal fibroblasts cultured with macrophage supernatant. Each dot in the bar charts represents a quadruplicate of the same plate. (**i**) Quantitation of the mRNA expression of *MMP1* in dermal fibroblasts cultured with macrophage supernatant. Each dot in the bar charts represents a quadruplicate of the same plate. Nuclei were stained with Hoechst (blue). All data are expressed as the mean value ± SD; n = 3–4 for control, M1 (LPS + IFN-γ), and M2 (IL-4 + IL-13). *$P < 0.05$ and **$P < 0.01$. To test for significance, Kruskal–Wallis test was used. Bar = 100 μm. hr, hour; IQR, interquartile range; LPS, lipopolysaccharide; MMP1, matrix metalloproteinase 1; ns, not significant.

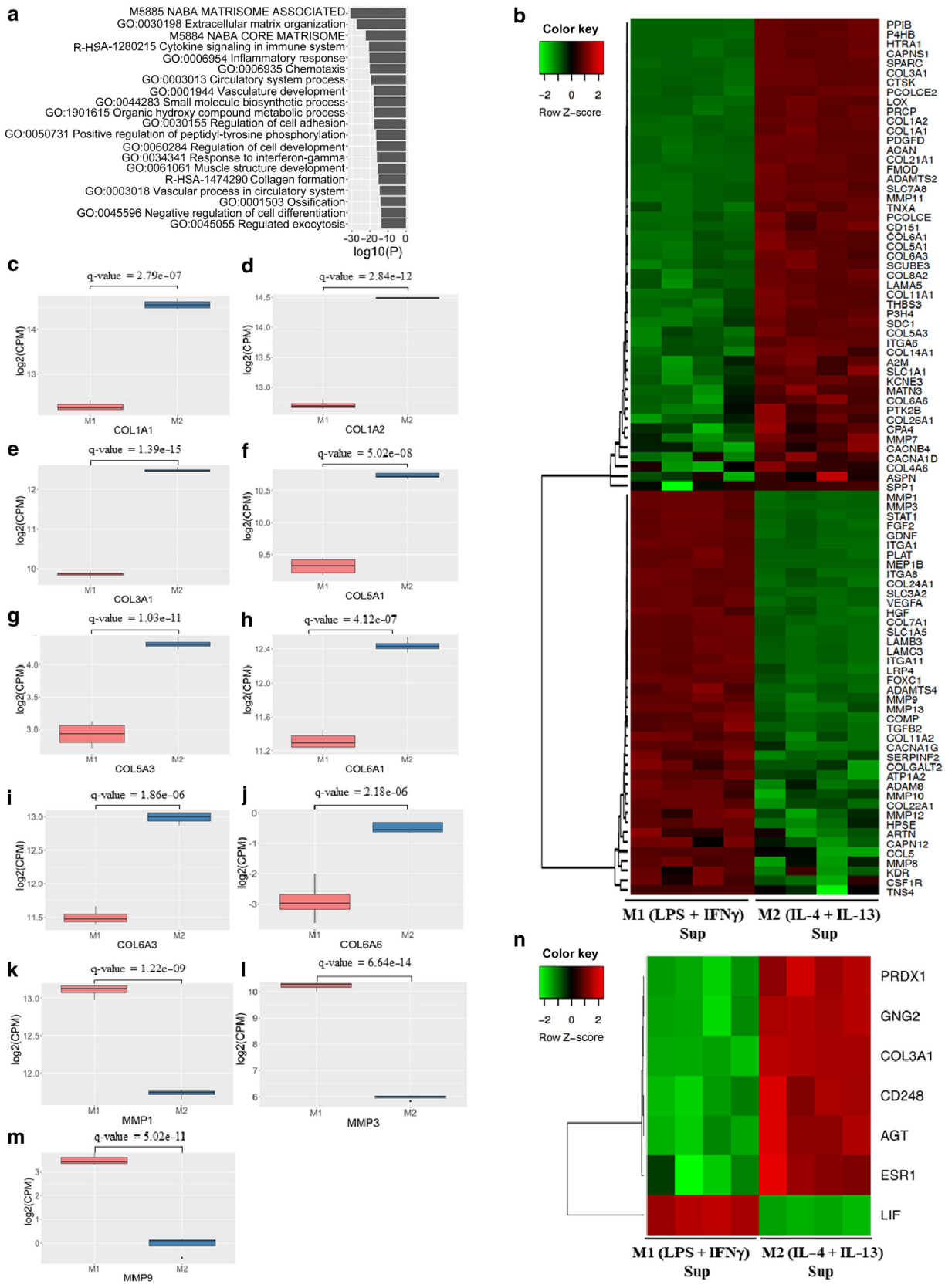

Figure 5. Differentially expressed gene analysis of dermal fibroblasts that were cultured with the M1 (LPS + IFN-γ) and M2 (IL-4 + IL-13) supernatants. (**a**) The top 20 results of enrichment analysis of the differentially expressed genes of dermal fibroblasts that were cultured with M1 (LPS + IFN-γ) and M2 (IL-4 + IL-13) supernatant. (**b**) Heatmap showing collagen formation–related differentially expressed genes. The green blocks show downregulated genes, and the red blocks show upregulated genes. The data are comparing four individual samples. (**c**–**m**) The differential expression of (**c**) *COL1A1*, (**d**) *COL1A2*, (**e**) *COL3A1*, (**f**) *COL5A1*, (**g**) *COL5A3*, (**h**) *COL6A1*, (**i**) *COL6A3*, (**j**) *COL6A6*, (**k**) *MMP1*, (**l**) *MMP3*, and (**m**) *MMP9*. Each box shows the median (central horizontal line) and

relationship between these collagens—especially types V and VI collagens—and macrophages in the skin has not been fully investigated. Therefore, to understand the mechanisms through which the M1/M2 balance affects collagen homeostasis with photoaging in more detail, we focused on the synthesis and assembly of these collagens. Interestingly, the M1/M2 ratio was negatively correlated with the abundance of types V and VI collagens but not with that of type III collagen. Some studies have reported that the abundance of type III collagen decreases only slightly or does not change with aging (Dumas et al., 1994; Vitellaro-Zuccarello et al., 1992). Indeed, we also found that the alteration of type III collagen with photoaging was much smaller than that of types I, V, and VI collagens. These results suggest that the M1/M2 balance may have a stronger effect on collagens that undergo large changes with photoaging. Type V collagen is the minor collagen that regulates fibril diameters and that is required for fibril nucleation of collagen by controlling the initiation of collagen fibril assembly (Wenstrup et al., 2004). Deficiencies in *COL5A1* and *COL5A2* cause classic Ehlers–Danlos syndrome, in which the skin is fragile, soft, and hyperextensible (Chanut-Delalande et al., 2004; Mak et al., 2016). Type VI collagen regulates dermal matrix assembly and collagen expression in dermal fibroblasts (Theocharidis et al., 2016), and it has been reported that variants in genes encoding type VI collagen cause myosclerosis myopathy, which is characterized by skin abnormalities (Lettmann et al., 2014; Sabatelli et al., 2011). However, the mechanism underlying the alteration of type VI collagen with photoaging has remained unknown. In this study, to determine the effects of M1 and M2 macrophages on collagen homeostasis, especially on that of types I, V, and VI collagens, dermal fibroblasts were cultured with the supernatant of M1 or M2 macrophages, and types I, V, and VI collagens were stained. We found a decrease in collagen fibrils consisting of types I, V, and VI collagens synthesized by dermal fibroblasts cultured with the supernatant of M1 macrophages, and the fibrils were fragmented, partially aggregated, and abnormal compared with those synthesized by dermal fibroblasts cultured in control and M2 medium. Our results, together with reported findings, suggest that shifts in the M1/M2 balance in photoaged skin may affect the synthesis and assembly of collagen fibrils through types I, V, and VI collagens and may reduce skin elasticity. This is evidence that skewing of the M1/M2 balance in sun-exposed human skin under steady-state conditions may affect collagen homeostasis.

Previously, we reported that the percentage of p16- and p21-positive senescent cells is significantly positively correlated with the M1/M2 ratio in the dermis of sun-exposed skin (Horiba et al., 2022). It has been reported that senescent fibroblasts secrete factors related to the senescence-associated secretory phenotype, including proteolytic enzymes that degrade collagen, and reduce the expression of genes involved in the formation of the extracellular matrix (Kim et al., 2022; Waldera Lupa et al., 2015; Wlaschek et al., 2021). These reports support our hypothesis and suggest that not only the direct effect of UV but also the effect of shifts in the M1/M2 balance induce dermal fibroblast senescence and that the related degradation of collagen results in fragile skin.

In this study, we focused on types I, V, and VI collagens and found that decreases in these collagens may cause abnormal fibrillogenesis in dermal fibroblasts. However, the precise mechanism through which the expression and fibrillogenesis of types I, V, and VI collagens are altered with photoaging of skin by the skewing of the M1/M2 balance requires further investigation. To investigate the mechanisms in more detail, we need to develop a model such as an ex vivo human skin model that lacks the candidate factors and that can be cultured for a long time to examine the aging process. Investigating the mechanism is expected to provide insight into the correlation between collagen homeostasis and macrophage balance in skin photoaging. In addition, although we focused on the dermis and dermal fibroblasts in this study, because other skin resident cells, such as epidermal keratinocytes, also affect skin photoaging, it is important and interesting to investigate the effect of the M1/M2 balance on the homeostasis of the whole area of skin to understand the mechanisms of skin photoaging.

In summary, although many reports have revealed the relationship between alterations in collagen and dermal fibroblasts in photoaged skin, the effect of immune cells on collagen is not fully understood. In this study, we showed that shifting the balance of M1 and M2 macrophages affected photoaged skin through types I, V, and VI collagens and provided a potential therapeutic target for preventing photoaging. Because alterations in collagen in photoaging may induce skin concerns such as wrinkles or sagging, these findings are potentially important in maintaining the QOL for aged people.

MATERIALS AND METHODS

Human skin tissue

Normal face skin samples were kindly provided by Obio, LLC (El Segundo, CA). The procedures complied with all applicable rules, laws, regulations, and ethical codes, and the samples were obtained with informed consent in compliance with all the regulations of the supplier. The samples were obtained from White young female cadavers (aged 25–43 years, mean = 34.2 years) and aged female cadavers (aged 62–88 years, mean = 74.5 years). During the experiments, all samples were identified with randomly assigned codes. Before the study, it was confirmed that Obio, LLC had obtained written informed consent. The use of human skin samples was also approved by the Ethics Committee. The certificate number of approval by the Ethics Committee is C10296.

Histochemistry and immunofluorescence staining of human skin tissue

The degree of solar elastosis was scored by performing Elastica van Gieson staining according to a previous report (Ogura et al., 2011), that is, 0 for no change, 1^+ for increase in number without

IQR, and whiskers represent the first and third quartiles of 1.5 × IQR. n = 4 for M1 and M2. CPM is the amount of expression corrected by the total number of mappings. (**n**) Heatmap showing fibroblast proliferation–related differentially expressed genes. The green blocks show downregulated genes, and the red blocks show upregulated genes. The data are comparing four individual samples. CPM, counts per million mapped reads; IQR, interquartile range; LPS, lipopolysaccharide; MMP, matrix metalloproteinase.

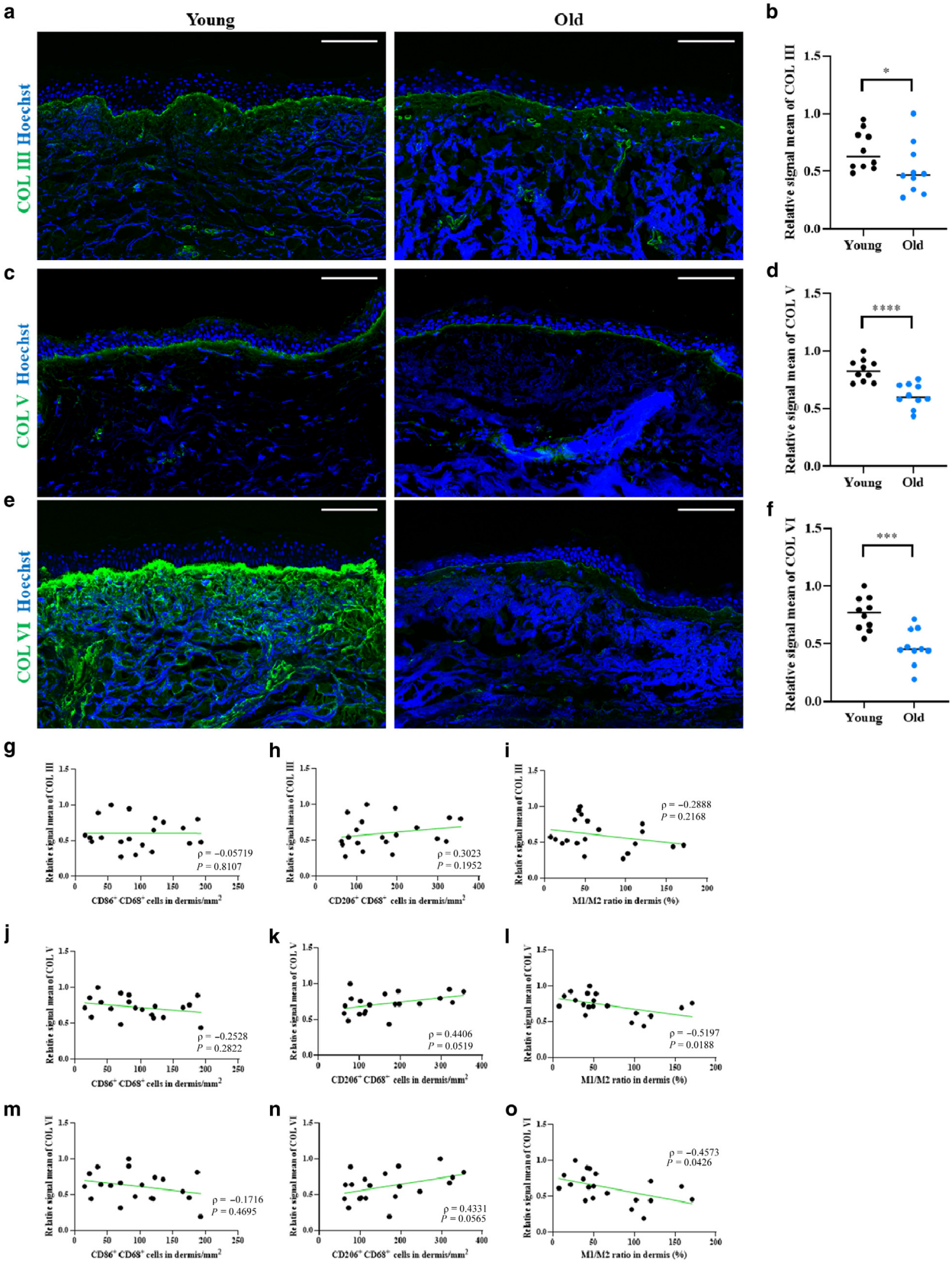

Figure 6. The amount of types V and VI collagens is related to the M1/M2 ratio in sun-exposed human skin. (**a**) Young (mean = 34.2 years) and aged (mean = 74.5 years) human skin was stained with anti–type III collagen (green) antibodies. (**b**) Quantitation of the relative mean signal of type III collagen in the papillary dermis. (**c**) Young and aged human skin was stained with anti–type V collagen (green) antibodies. (**d**) Quantitation of the relative mean signal of type V collagen in the papillary dermis. (**e**) Young and aged human skin was stained with anti–type VI collagen (green) antibodies. (**f**) Quantitation of the relative mean signal of type VI collagen in the papillary dermis. Correlation between the relative mean signal of type III collagen and (**g**) the number of M1 macrophages in the papillary

thickening; 2^+ for greater hyperplasia with thickening and curling; 3^+ for marked hyperplasia with thickening and curling and frequent branching; and 4^+ for complete replacement of the dermis by a dense tangle of thickened, disorderly fibers, accompanied by disorganization into murky amorphous masses. The sections were counterstained with H&E. The human skin samples were prepared and stained as described previously (Horiba et al., 2022). The samples were stained with primary antibodies against CD206 (1:200, AF2534, R&D Systems, Minneapolis, MN), CD68 (1:100, ab955, Abcam, Cambridge, United Kingdom), CD86 (1:50, AF141NA, R&D Systems), type I collagen (1:500, ab6308, Abcam), type III collagen (1:200, 600-401-105S, Rockland Immunochemicals, Limerick, PA), type V collagen (1:100, AM10159PU-N, OriGene, Rockville, MD), and type VI collagen (1:400, MAB1944, MilliporeSigma, Temecula, CA). In the dermis, positive cells located within 200 μm of the epidermal border were evaluated. The staining intensity of collagen within 200 μm of the epidermal border was analyzed using ImageJ software (National Institutes of Health, Bethesda, MD). For each sample, images from more than five high-power fields (magnification ×200) in total were assessed. Positive cells (cells/mm^2) were determined by counting the positive cells in all fields (>5 fields) and dividing by the gross area.

Quantification of the SHG signals in human skin tissue

The SHG light intensity of collagen was imaged under a multiphoton microscope (FVMPE-RS, Olympus, Tokyo, Japan), as reported previously (Sugita et al., 2021). Briefly, a laser (wavelength = 800 nm, pulse width = 100 fs, repeated frequency = 80 MHz) was applied to the prepared samples through a ×25 objective lens (numerical aperture = 1.05, XLPLN25XW, Olympus). The generated SHG light was observed using a bandpass filter (400 ± 5 nm). All specimens were prepared as 10.0-mm tissue slices and observed under the same conditions (laser transmissivity = 10.0 %, sampling speed = 2.0 ms/pixel, image resolution = 2.486 mm/pixel). In the dermis, the SHG intensity within 200 μm of the epidermal border was evaluated and analyzed using ImageJ software (National Institutes of Health). For each sample, images from >5 high-power fields (magnification ×200) were assessed.

Cell preparations

THP-1 cells were obtained from ATCC (Manassas, VA) and were cultured in RPMI 1640 medium (Nacalai Tesque, Kyoto, Japan) supplemented with 10% fetal bovine serum, 1 mM sodium pyruvate, and 2 mM L-glutamine at 37 °C. The cells were differentiated into M0, M1, and M2 macrophages using a standard protocol as described previously (Tjiu et al., 2009) and called M1 (LPS + IFN-γ) and M2 (IL-4 + IL-13), respectively, in this study. Normal human newborn dermal fibroblasts (Kurabo Industries, Osaka, Japan) were cultured in DMEM (Invitrogen, Carlsbad, CA) supplemented with 10% fetal bovine serum, 100 units/ml penicillin, and 100 mg/ml streptomycin at 37 °C. Fibroblasts from passages 5–10 were used for all experiments.

Ex vivo human skin model and culture

M1 (LPS + IFN-γ) or M2 (IL-4 + IL-13) derived from THP-1 cells were seeded at a density of 5×10^5 cells/well in 12-well culture plates (Corning, Corning, NY) and cultured in RPMI 1640 medium (Nacalai Tesque) supplemented with 10% fetal bovine serum, 1 mM sodium pyruvate, and 2 mM L-glutamine at 37 °C for 24 hours. The medium was removed, and the medium for the NativeSkin model (Genoskin, Toulouse, France) was added to M1 or M2 macrophages derived from THP-1 cells, and the NativeSkin models (Genoskin) were placed in the wells. NativeSkin models (aged 25–38 years, mean = 32.3 years) were cultured at 37 °C for 6 days.

RNA-sequencing analysis

Total RNA was extracted from dermal fibroblasts that were cultured with M1 (LPS + IFN-γ) or M2 (IL-4 + IL-13) supernatant as described earlier. Sequencing libraries were prepared using a TruSeq Stranded mRNA Library prep kit (Illumina, San Diego, CA), TurSeq RNA UD Indexes (Illumina), and Agilent XT-Auto System (Agilent, Santa Clara, CA) according to the TruSeq Stranded mRNA Reference Guide, version 00 (Illumina), and were sequenced on an Illumina NovaSeq 6000 platform with 150-bp paired-end reads according to the NovaSeq 6000 Sequencing System Guide, version 11 (Illumina), and bcl2fastq conversion Software, version 2.20 Software Guide (Illumina). Sequenced reads were mapped onto the human reference genome GRCh37/hg19 using STAR (Spliced Transcripts Alignment to a Reference), version 2.6.0c (Dobin et al., 2013), and the results were calculated and annotated using the Genedata Profiler Genome (version 13.0.11). Comparative transcriptome analysis was performed using edgeR (version 3.20.9) (Robinson et al., 2010), and the calculated *P*-values were corrected for multiple comparisons using the Benjamini–Hochberg method to calculate q-values. Q-values < 0.05 were considered differentially expressed genes. Hierarchical cluster analysis was performed using the hclust package in the R statistical analysis program (version 3.6.2) (R Core Team, 2019). Heatmaps were drawn using heatmap2 in the gplots package (version 3.1.1) (Warnes et al., 2019). Enrichment analysis of the selected genes by biological function was performed using Metascape (Zhou et al., 2019).

Real-time RT-PCR

Total RNA was isolated from normal human newborn dermal fibroblasts (Kurabo Industries) using a commercial kit (RNeasy Mini Kit, Qiagen, Chatsworth, CA) according to the manufacturer's instructions. Real-time RT–PCR analysis of *COL1A1*, *COL1A2*, *MMP1*, and housekeeping gene *GAPDH* was performed using a TaqMan RNA-to C_T 1-Step Kit (Applied Biosystems, Foster City, CA) according to the manufacturer's instructions. The relative quantification value of COL1A1, COL1A2, and MMP1 were normalized to endogenous GAPDH. Gene-specific probes labeled with fluorescein amidites were purchased from Applied Biosystems.

Quantification of procollagen type I C-peptide and immunostaining of types I, V, and VI collagens

M1 (LPS + IFN-γ) and M2 (IL-4 + IL-13) derived from THP-1 cells were cultured with RPMI 1640 medium supplemented with 0.5%

dermis, (**h**) the number of M2 macrophages in the papillary dermis, and (**i**) the M1/M2 ratio in young and aged skin samples. Correlation between the relative mean signal of type V collagen and (**j**) the number of M1 macrophages in the papillary dermis, (**k**) the number of M2 macrophages in the papillary dermis, and (**l**) the M1/M2 ratio in young and aged skin samples. Correlation between the relative mean signal of type VI collagen and (**m**) the number of M1 macrophages in the papillary dermis, (**n**) the number of M2 macrophages in the papillary dermis, and (**o**) the M1/M2 ratio in young and aged skin samples. Nuclei were stained with Hoechst (blue). n = 10 in both the young and aged groups. *$P < 0.05$, ***$P < 0.001$, and ****$P < 0.0001$. To test for significance, the Mann–Whitney *U* test was used. To test the significance of the scatter plots, Spearman's rank correlation coefficient was used. Bar = 100 μm. ns, not significant.

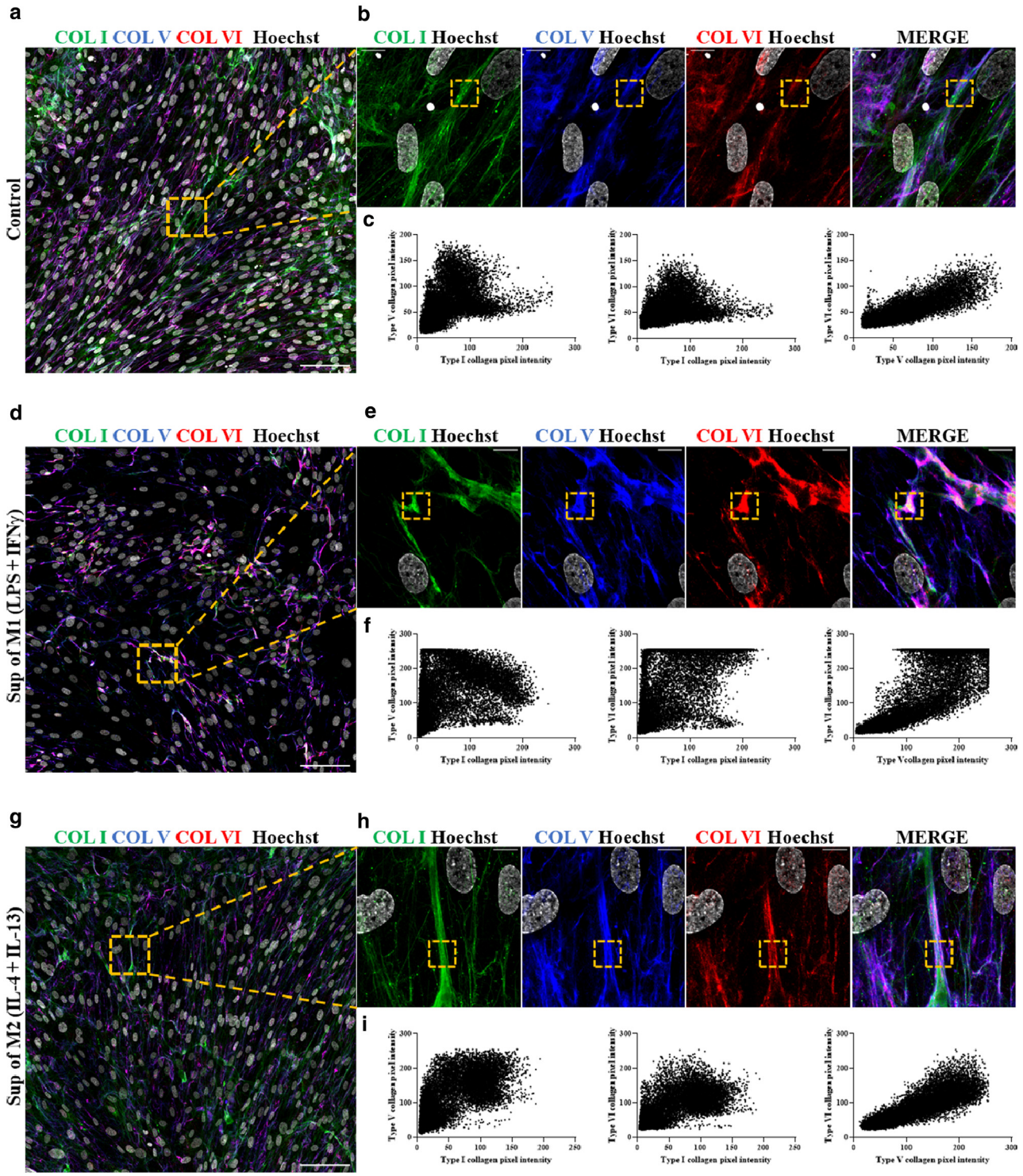

Figure 7. Collagen fibril formation is regulated by the M1/M2 balance of macrophages. Representative immunofluorescence staining of type I collagen (green), type V collagen (blue), and type VI collagen (red) in dermal fibroblasts (**a**) cultured with control medium; (**b**) enlarged view of **a**. (**c**) Scatterplot of green, blue, and red pixel intensities of the ROI shown in **b**. (**d**) Representative immunofluorescence staining of type I collagen (green), type V collagen (blue), and type VI collagen (red) in dermal fibroblasts cultured with M1 (LPS + IFN-γ) supernatant; (**e**) enlarged view of **d**. (**f**) Scatterplot of green, blue, and red pixel intensities of the ROI shown in **e**. (**g**) Representative immunofluorescence staining of type I collagen (green), type V collagen (blue), and type VI collagen (red) in dermal fibroblasts cultured with M2 (IL-4 + IL-13) supernatant; (**h**) enlarged view of **g**. (**i**) Scatterplot of green, blue, and red pixel intensities of the ROI shown in **h**. Nuclei were stained with Hoechst (gray). Bar = 100 μm or 10 μm in the enlarged view. LPS, lipopolysaccharide; ROI, region of interest.

fetal bovine serum, 500 mM ascorbic acid, and 2 mM L-glutamine at 37 °C for 48 hours, and the supernatants were collected. Then, the supernatants were added to normal human newborn foreskin dermal fibroblasts (Kurabo Industries). Seventy-two to 96 hours after the administration of M1 (LPS + IFN-γ) or M2 (IL-4 + IL-13) supernatant, the supernatants of the normal human newborn foreskin dermal

fibroblasts (Kurabo Industries) were collected, and the abundance of procollagen type I C-peptide was analyzed using a Procollagen Type I C-peptide EIA kit (Takara Shuzo, Kyoto, Japan) according to the manufacturer's instructions. In addition, the cells were incubated overnight at 4 °C with antibodies against type I collagen (1:100, CL50111AP-1, Cedarlane labs, Burlington, Canada), type I collagen (1:100, ab24821, Abcam), type V collagen (1:100, ab7046, Abcam), and type VI collagen (1:100, MAB1944, MilliporeSigma) and then with corresponding secondary antibodies labeled with Alexa Fluor 488, 568, and 647. Scatterplots of pixel intensity were analyzed using ImageJ software (National Institutes of Health). Nuclear counterstaining was performed with Hoechst. As a control, dermal fibroblasts were incubated for 72–96 hours in RPMI 1640 medium supplemented with 0.5% fetal bovine serum, 500 mM ascorbic acid, and 2 mM L-glutamine.

Statistical analysis

The data were analyzed using GraphPad Prism (GraphPad Software, La Jolla, CA). Column scatter plots show the mean value. To compare cell counts in the skin, the Mann–Whitney *U* test was used. To compare the intensity of type I collagen, Friedman's test with multiple comparisons was used. To compare mRNA expression, procollagen expression Kruskal–Wallis test was used. For scatter plots, Spearman's rank correlation coefficient was used. $P < 0.05$ was considered to indicate a significant difference. For the statistical analysis of the bulk RNA, we used a program called edgeR, as previously described (Robinson et al., 2010). EdgeR performs multiple testing correction using Benjamini–Hochberg in the edgeR process.

Data availability statement

Datasets related to this article can be found at https://ddbj.nig.ac.jp/resource/sra-submission/DRA014322/, hosted at The DNA Data Bank of Japan (under accession number DRA014322).

ORCIDs

Satoshi Horiba: http://orcid.org/0000-0002-7047-0097
Munetaka Kawamoto: http://orcid.org/0000-0003-3554-8407
Ryozo Tobita: http://orcid.org/0000-0002-6886-453X
Ryota Kami: http://orcid.org/0000-0001-5052-6068
Yuki Ogura: http://orcid.org/0000-0001-7475-5826
Junichi Hosoi: http://orcid.org/0000-0002-8534-9652

CONFLICT OF INTEREST

The authors state no conflict of interest.

ACKNOWLEDGMENTS

SH, RK, RT, YO, JH, and MK were supported by Shiseido. The authors thank Tatsuya Hasegawa, Mika Sawane, Taiki Tsutsui, Chie Yasuda, Hiroyuki Aoki, Shunsuke Iriyama, Kiyoshi Sato, and Kentaro Kajiya for valuable discussions. Normal face skin samples were kindly provided by Obio, LLC (El Segundo, CA). The procedures complied with all applicable rules, laws, regulations, and ethical codes, and the samples were obtained with informed consent in compliance with all the regulations of the supplier. During the experiments, all samples were identified with randomly assigned codes. Before the study, it was confirmed that Obio had obtained written informed consent. The use of human skin samples was also approved by the Ethics Committee of Shiseido. The certificate number of approval by the Shiseido Ethics Committee is C10296.

AUTHOR CONTRIBUTIONS

Conceptualization: SH, JH; Data Curation: SH, MK, RT, RK, YO, JH; Formal Analysis: SH, MK, RT, RK; Funding Acquisition: SH, MK, RT, RK, YO, JH; Investigation: SH, MK, RT, RK; Methodology: SH, MK, RT, RK, YO, JH; Project Administration: SH; Resources: SH, MK, RT, RK, YO, JH; Supervision: SH, JH; Validation: SH, MK, RT, RK, YO, JH; Visualization: SH, MK, RT, RK, JH; Writing - Original Draft Preparation: SH, MK and JH; Writing - Review and Editing: SH, MK, RT, RK, YO, JH

REFERENCES

Bekhouche M, Colige A. The procollagen N-proteinases ADAMTS2, 3 and 14 in pathophysiology. Matrix Biol 2015;44–46:46–53.

Bonod-Bidaud C, Roulet M, Hansen U, Elsheikh A, Malbouyres M, Ricard-Blum S, et al. In vivo evidence for a bridging role of a collagen V subtype at the epidermis-dermis interface. J Invest Dermatol 2012;132:1841–9.

Bradshaw AD, Puolakkainen P, Dasgupta J, Davidson JM, Wight TN, Helene Sage E. SPARC-null mice display abnormalities in the dermis characterized by decreased collagen fibril diameter and reduced tensile strength. J Invest Dermatol 2003;120:949–55.

Chanut-Delalande H, Bonod-Bidaud C, Cogne S, Malbouyres M, Ramirez F, Fichard A, et al. Development of a functional skin matrix requires deposition of collagen V heterotrimers. Mol Cell Biol 2004;24:6049–57.

Cole MA, Quan T, Voorhees JJ, Fisher GJ. Extracellular matrix regulation of fibroblast function: redefining our perspective on skin aging. J Cell Commun Signal 2018;12:35–43.

Dobin A, Davis CA, Schlesinger F, Drenkow J, Zaleski C, Jha S, et al. STAR: ultrafast universal RNA-seq aligner. Bioinformatics 2013;29:15–21.

Dumas M, Chaudagne C, Bonté F, Meybeck A. In vitro biosynthesis of type I and III collagens by human dermal fibroblasts from donors of increasing age. Mech Ageing Dev 1994;73:179–87.

El-Domyati M, Attia S, Saleh F, Brown D, Birk DE, Gasparro F, et al. Intrinsic aging vs. photoaging: a comparative histopathological, immunohistochemical, and ultrastructural study of skin. Exp Dermatol 2002;11:398–405.

Fisher GJ, Sachs DL, Voorhees JJ. Ageing: collagenase-mediated collagen fragmentation as a rejuvenation target. Br J Dermatol 2014;171:446–9.

Fisher GJ, Wang ZQ, Datta SC, Varani J, Kang S, Voorhees JJ. Pathophysiology of premature skin aging induced by ultraviolet light. N Engl J Med 1997;337:1419–28.

Fleischmajer R, MacDonald ED, Perlish JS, Burgeson RE, Fisher LW. Dermal collagen fibrils are hybrids of type I and type III collagen molecules. J Struct Biol 1990;105:162–9.

Fligiel SE, Varani J, Datta SC, Kang S, Fisher GJ, Voorhees JJ. Collagen degradation in aged/photodamaged skin in vivo and after exposure to matrix metalloproteinase-1 in vitro. J Invest Dermatol 2003;120:842–8.

Gelse K, Pöschl E, Aigner T. Collagens–structure, function, and biosynthesis. Adv Drug Deliv Rev 2003;55:1531–46.

Gordon JR, Brieva JC. Images in clinical medicine. Unilateral dermatohelioisis. N Engl J Med 2012;366:e25.

Horiba S, Kami R, Tsutsui T, Hosoi J. IL-34 downregulation-associated M1/M2 macrophage imbalance is related to inflammaging in sun-exposed human skin. JID Innov 2022;2:100112.

Kagan HM, Li W. Lysyl oxidase: properties, specificity, and biological roles inside and outside of the cell. J Cell Biochem 2003;88:660–72.

Kim H, Jang J, Song MJ, Park CH, Lee DH, Lee SH, et al. Inhibition of matrix metalloproteinase expression by selective clearing of senescent dermal fibroblasts attenuates ultraviolet-induced photoaging. Biomed Pharmacother 2022;150:113034.

Kligman AM. Early destructive effect of sunlight on human skin. JAMA 1969;210:2377–80.

Knipper JA, Willenborg S, Brinckmann J, Bloch W, Maaß T, Wagener R, et al. Interleukin-4 receptor α signaling in myeloid cells controls collagen fibril assembly in skin repair. Immunity 2015;43:803–16.

Lettmann S, Bloch W, Maaß T, Niehoff A, Schulz JN, Eckes B, et al. Col6a1 null mice as a model to study skin phenotypes in patients with collagen VI related myopathies: expression of classical and novel collagen VI variants during wound healing. PLoS One 2014;9:e105686.

Mahdavian Delavary B, van der Veer WM, van Egmond M, Niessen FB, Beelen RH. Macrophages in skin injury and repair. Immunobiology 2011;216:753–62.

Mak KM, Png CY, Lee DJ. Type V collagen in health, disease, and fibrosis. Anat Rec (Hoboken) 2016;299:613–29.

McCabe MC, Hill RC, Calderone K, Cui Y, Yan Y, Quan T, et al. Alterations in extracellular matrix composition during aging and photoaging of the skin. Matrix Biol Plus 2020;8:100041.

Ogura Y, Kuwahara T, Akiyama M, Tajima S, Hattori K, Okamoto K, et al. Dermal carbonyl modification is related to the yellowish color change of photo-aged Japanese facial skin. J Dermatol Sci 2011;64:45–52.

Pittayapruek P, Meephansan J, Prapapan O, Komine M, Ohtsuki M. Role of matrix metalloproteinases in photoaging and photocarcinogenesis. Int J Mol Sci 2016;17:868.

Quan T, Little E, Quan H, Qin Z, Voorhees JJ, Fisher GJ. Elevated matrix metalloproteinases and collagen fragmentation in photodamaged human skin: impact of altered extracellular matrix microenvironment on dermal fibroblast function. J Invest Dermatol 2013;133:1362–6.

R Core Team. R: a language and environment for statistical computing. Vienna, Austria: R Foundation for Statistical Computing; 2019.

Rentz TJ, Poobalarahi F, Bornstein P, Sage EH, Bradshaw AD. SPARC regulates processing of procollagen I and collagen fibrillogenesis in dermal fibroblasts. J Biol Chem 2007;282:22062–71.

Rittié L, Fisher GJ. UV-light-induced signal cascades and skin aging. Ageing Res Rev 2002;1:705–20.

Rittié L, Fisher GJ. Natural and sun-induced aging of human skin. Cold Spring Harb Perspect Med 2015;5:a015370.

Robinson MD, McCarthy DJ, Smyth GK. edgeR: a Bioconductor package for differential expression analysis of digital gene expression data. Bioinformatics 2010;26:139–40.

Sabatelli P, Gara SK, Grumati P, Urciuolo A, Gualandi F, Curci R, et al. Expression of the collagen VI α5 and α6 chains in normal human skin and in skin of patients with collagen VI-related myopathies. J Invest Dermatol 2011;131:99–107.

Sonoki A, Okano Y, Yoshitake Y. Dermal fibroblasts can activate matrix metalloproteinase-1 independent of keratinocytes via plasmin in a 3D collagen model. Exp Dermatol 2018;27:520–5.

Sugita S, Suzumura T, Nakamura A, Tsukiji S, Ujihara Y, Nakamura M. Second harmonic generation light quantifies the ratio of type III to total (I + III) collagen in a bundle of collagen fiber. Sci Rep 2021;11:11874.

Theocharidis G, Drymoussi Z, Kao AP, Barber AH, Lee DA, Braun KM, et al. Type VI collagen regulates dermal matrix assembly and fibroblast motility. J Invest Dermatol 2016;136:74–83.

Tjiu JW, Chen JS, Shun CT, Lin SJ, Liao YH, Chu CY, et al. Tumor-associated macrophage-induced invasion and angiogenesis of human basal cell carcinoma cells by cyclooxygenase-2 induction [published correction in J Invest Dermatol 2018;138:471] J Invest Dermatol 2009;129:1016–25.

Varani J, Perone P, Fligiel SE, Fisher GJ, Voorhees JJ. Inhibition of type I procollagen production in photodamage: correlation between presence of high molecular weight collagen fragments and reduced procollagen synthesis. J Invest Dermatol 2002;119:122–9.

Vitellaro-Zuccarello L, Garbelli R, Rossi VD. Immunocytochemical localization of collagen types I, III, IV, and fibronectin in the human dermis. Modifications with ageing. Cell Tissue Res 1992;268:505–11.

Waldera Lupa DM, Kalfalah F, Safferling K, Boukamp P, Poschmann G, Volpi E, et al. Characterization of skin aging-associated secreted proteins (SAASP) produced by dermal fibroblasts isolated from intrinsically aged human skin. J Invest Dermatol 2015;135:1954–68.

Warnes GR, Bolker B, Bonebakker L, Gentleman R, Liaw A, Lumley T, et al. gplots: various R programming tools for plotting data. https://cran.r-project.org/web/packages/gplots/gplots.pdf; 2019. (accessed July 20, 2023).

Wenstrup RJ, Florer JB, Brunskill EW, Bell SM, Chervoneva I, Birk DE. Type V collagen controls the initiation of collagen fibril assembly. J Biol Chem 2004;279:53331–7.

Wlaschek M, Maity P, Makrantonaki E, Scharffetter-Kochanek K. Connective tissue and fibroblast senescence in skin aging. J Invest Dermatol 2021;141:985–92.

Wynn TA, Vannella KM. Macrophages in tissue repair, regeneration, and fibrosis. Immunity 2016;44:450–62.

Xia W, Hammerberg C, Li Y, He T, Quan T, Voorhees JJ, et al. Expression of catalytically active matrix metalloproteinase-1 in dermal fibroblasts induces collagen fragmentation and functional alterations that resemble aged human skin. Aging Cell 2013;12:661–71.

Zhou Y, Zhou B, Pache L, Chang M, Khodabakhshi AH, Tanaseichuk O, et al. Metascape provides a biologist-oriented resource for the analysis of systems-level datasets. Nat Commun 2019;10:1523.